



Laser-aided curing of a GnP/epoxy nanocomposite optimised by multiscale finite element analysis

Asimina Manta¹ | Constantinos Soutis² | Matthieu Gresil^{1,2}

¹i-composites Laboratory, School of Materials, University of Manchester, Manchester, UK

²Aerospace Research Institute, Faculty of Science and Engineering, University of Manchester, Manchester, UK

Correspondence

Constantinos Soutis, Aerospace Research Institute, Faculty of Science and Engineering, University of Manchester, James Lighthill Building, Sackville Street, Manchester M1 3NJ, UK.

Email: constantinos.soutis@manchester.ac.uk

Funding information

President's Doctoral Scholar (PDS) Awards; University of Manchester, Grant/Award Number: President's Doctoral Scholar (PDS) Awards scheme

Abstract

In this work, the possibility of laser-aided curing of graphene nanoplatelet (GnP)/epoxy nanocomposites is explored by means of finite element analysis. A multiscale and multiphysics analysis is performed to identify and optimise critical manufacturing parameters—laser speed and power. The proposed model is parametrically studied, and its results are thoroughly discussed in terms of polymerisation degree and temperature field depth. Finally, the laser scanning of a specimen was conducted, and the polymerisation performance was recorded.

KEYWORDS

graphene nanoparticles, polymer, nanocomposite, laser, polymerisation, multiscale, finite element analysis

1 | BACKGROUND

The manufacturing process of any composite material structure exhibits important challenges, including the development of time and cost-effective methods, enabling mass production with high repeatability in the products' specification. The ability of the carbon-based nanofillers to absorb light wavelengths could be exploited in eco-friendly manufacturing processes based on radiation and laser curing techniques. Especially, graphene is a two-dimensional material with carbon atoms in a honeycomb lattice. It has many potential applications thanks to its unique electrical, mechanical, chemical, and optical properties.^{1–3} The optical transmittance of multilayer graphene films up to 65 layers thick was studied in the work of Zhu et al.,⁴ finding the optical transmission through graphene films in the visible region be solely determined by the number of graphene layers. The incorporation of periodic gold nanoparticles arrays into graphene-based photodetectors to enhance and tune light absorption of graphene was found in the work of Zhu et al.⁵ The significance of the ability of graphene to absorb the light was highly utilised by direct absorption solar collectors (DASCs) used in solar energy conversion applications.^{6–8}

Furthermore, laser applications have received an increasing attention for a wide variety of applications such as scientific, military, medicine, industries, and other fields due to its excellent quality with high productivity and flexibility.⁹ Main variable parameters in this process are the power and diameter of the laser beam as it moves across the surface of a workpiece. A number of models have been developed to simulate the laser treatment of a surface and study the effect of the process variables and the quality of the product. A three-dimensional finite element modelling of laser surface modification is presented in the work of Labudovic et al.,¹⁰ while in Bachy and Franke,¹¹ a three-dimensional numerical heat transfer model was employed to simulate the laser structuring of polymer substrate material in the three-dimensional molded interconnect device (3D MID), which is used in the advanced multifunctional

applications. In terms of graphene ability to absorb light, it is combined with laser heating in the simulation of the next study.¹² In specific, it investigates heat transfer on the multilayered structure with graphene overcoat induced by laser heating.

Knowledge from all these seemingly irrelevant works has been combined to form a multiscale finite element model¹³⁻¹⁶ to simulate the curing of graphene/polymer nanocomposite. At first, a unit cell consisting of the GnP particle and the liquid epoxy is considered to determine the temperature-dependent thermal conductivity and specific enthalpy. Afterwards, a macroscopic specimen, on which the unit cell obtained properties are distributed, is subjected to laser loading conditions, and the effect of the laser speed and power on the polymerisation degree and temperature field depth are found. Considering all the selected data, it will be shown that the polymerisation degree and the penetration of the temperature field increase with decreasing laser speed and increasing laser power, forming a scheme of highly customised manufacturing process in accordance to the specimen thickness and production line rate.

2 | MULTISCALE FINITE ELEMENT MODEL

The unit cell is a square plate consisting of the GnP particle and its surrounding liquid polymer. Between the GnP and the polymer, thermal contact elements were applied, simulating the interfacial thermal resistance (Figure 1A). The geometry was built with SOLID70 3D 8-node thermal solid elements. The interfacial resistance was modelled through CONT174—3D 8-node surface to surface contact element—and TARGE170—3D target segment—and it was approached by a temperature dependent Kapitza resistance. The unit cell side was divided with 40 elements, the filler diameter was discretised with 20 elements, while the filler circumference had 80 elements. There were two elements per filler thickness, too. For both phases, temperature-dependent properties were assumed. For the case of epoxy, the specific reaction enthalpy of a two-component resin (Biresin CR170/CH150-3) was modelled for temperature rate of 1 K/min as recorded.¹⁷ The thermal conductivity exhibited the same trend as the specific reaction enthalpy with $K = 0.06$ W/mK when the polymerisation degree is 0 (liquid) and $K = 0.19$ W/mK when the polymer is fully polymerised (solid). Accordingly, the applied response for GnP was retrieved by Pop et al.¹⁸ The temperature-dependent thermal properties were obtained at this level, to be afterwards distributed in the specimen model. To obtain the in-plane thermal conductivity, a temperature difference was applied to two opposite sides of the unit cell, while the rest ones were insulated. Accordingly, the through-the-thickness thermal conductivity was calculated through a temperature difference on the top and bottom surfaces, and the side surfaces were insulated too. The heat flow was recorded in every case, and the thermal conductivity was calculated through the law of heat conduction.¹⁵ The specific reaction enthalpy was simulated by applying a temperature gradient on all sides of the unit cell and recording the transient response.

The specimen is a rectangular cuboid with length of 10 mm, width of 5 mm, and thickness of 1 mm (Figure 1B). It was built with SOLID70 3D 8-node thermal solid elements. The elements had a size of $0.05 \times 0.05 \times 0.05$ mm³. Temperature-dependent material properties, previously obtained in the unit cell, were distributed randomly in the specimen volume, to approach the nanocomposite architecture. The initial temperature was set to the room temperature (20°C). To simulate the heat offered by the laser, the laser beam was modelled as a heat flux (heat rate per area) applied on a circular area with radius $r_{\text{laser}} = 200$ μm. The maximum laser power was 1.25 W, and the laser speed ranged

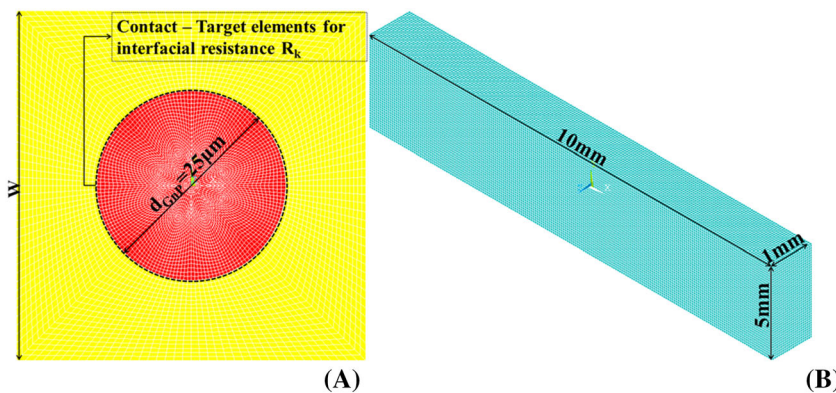


FIGURE 1 A, Unit cell top view with unit cell width w and GnP particle diameter $d_{\text{GnP}} = 25$ μm. B, Cuboid specimen model of nanocomposite with surface of 10 mm \times 5 mm and thickness of 1 mm

between 5 and 300 mm/s. On the rest area—which is the area not being loaded with the laser heat flux—convection was applied to simulate the cooling of the surface of the rest material. The convection coefficient was set to $10 \text{ W/m}^2\text{K}$ (air with zero flow velocity) while the room temperature was set to 20°C .

3 | RESULTS

A parametrical study was conducted on the effect of laser parameters (speed and power) on the polymerisation degree obtained and the depth of the temperature field. In each case, a single scan on the length of the specimen was applied. The polymerisation degree is presented in function of the position of the laser x . The coordinate system is set to the middle of the specimen.

In Figure 2, the effect of laser parameters (speed and power) on the polymerisation degree of nanocomposites with weight fractions of 5% is presented. In every case, the polymerisation degree is increased with laser power as a result of increased offered heat. On the other hand, the polymerisation decreases with laser speed. When the laser beam scans quickly the specimen, smaller amount of heat per area is offered compared to slower scans, therefore leading to lower polymerisation degree.

One of the most crucial manufacturing parameters is the temperature field depth achieved, deciding the thickness of the final product. The effect of the laser power and speed on the temperature field depth was studied for 1.0 to 12.5 wt% nanocomposites. The depth was decided as the distance from the top/heated surface to the point where the temperature was raised to 5% from the initial one ($\approx 308 \text{ K}$). The through-the-thickness temperature field was measured at the centre of the specimen at the middle of the process. In Figure 3, the obtained results are presented. In Figure 3A, the depth was recorded for 1.5% to 50% laser power and laser speed of 5 mm/s, while in Figure 3B, the laser power was kept constant to 1.5%. As expected, the temperature field depth increases with increasing laser power and decreasing laser speed. The maximum sample thickness could be 0.20 mm (200 μm) when the laser power is 10% and the laser speed is 5 mm/s.

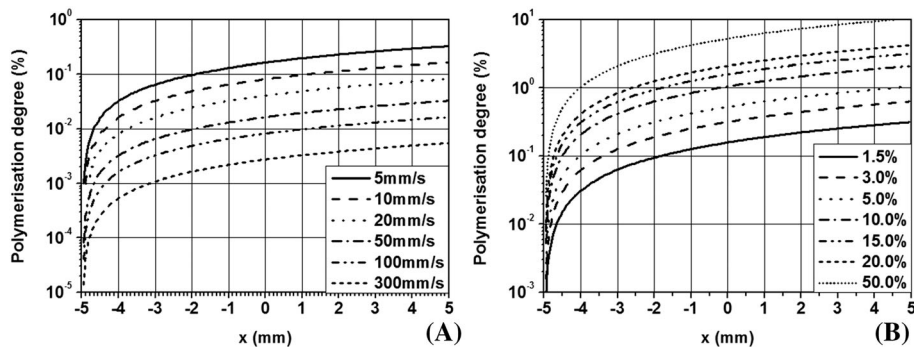


FIGURE 2 Effect of (A) laser speed and (B) laser power on polymerisation degree of 5.0 wt% GnP/epoxy nanocomposite. The laser power was set to 1.5% for results in (A) and the laser speed was 5 mm/s for (B)

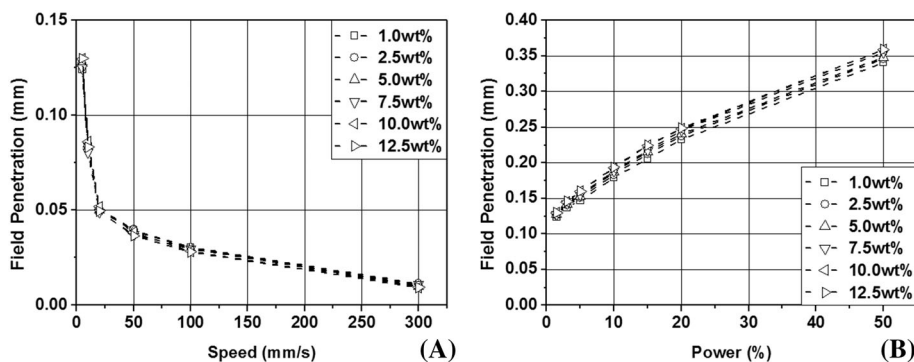


FIGURE 3 Temperature field depth as a function of (A) laser power and (B) speed for 1.0 to 12.5 wt% GnP/epoxy

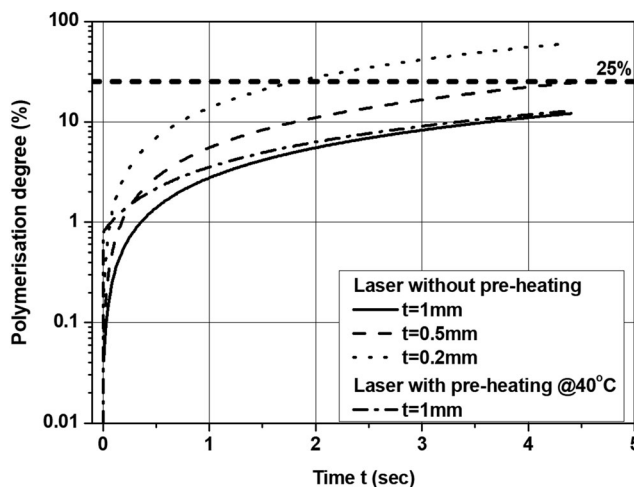


FIGURE 4 Polymerisation degree on scanning area of 1 mm × 1 mm with different thicknesses and including material preheating effect in function of time

Considering the above findings, this laser curing process could be efficient for the manufacturing of nanocomposite films and coatings.

Finally, the laser scanning of an area of 1 mm × 1 mm in the centre of a specimen 2 mm × 2 mm was conducted. A central area was chosen on the material to avoid any edge effects. The scanning was applied to specimens with different thicknesses—1, 0.5, and 0.2 mm—and the laser had a speed of 5 mm/s and power set at 5%, while the nanofluid was loaded with 5 wt% GnP. The design of the laser curing would be successful, if by the end of the process, the polymerisation degree of the volume/mass would be at 25%.

The polymerisation degree achieved for each case is presented in Figure 4. As it would be expected, the polymerisation degree is increasing with decreasing thickness, while for $t = 0.5$ mm, the 25% of the specimen was already polymerised. This observation does not necessarily indicate that the scanned area was cured through its thickness, but also, the nearby volumes might have been polymerised as a result of the heat transfer. For specimen thickness $t = 0.2$ mm, the polymerisation degree reaches 60% indicating clearly the polymerisation of volumes that were not scanned by the laser. For comparison reasons, the specimen with thickness of 1 mm was laser cured with preheating the material at 40°C. It could be seen that material preheating has a minor effect on the polymerisation degree.

4 | CONCLUSIONS

The laser-aided curing of graphene/epoxy nanocomposites was simulated by a multiscale finite element model. The temperature-dependent thermal properties were obtained at unit cell, and then, the polymerisation performance of the material was calculated for different filler loading and manufacturing parameters (laser speed and power). A scheme was created on the customisation of the manufacturing process, accounting for the laser speed and power, and the material thickness. By decreasing the laser speed, the thickness of the polymerised material was increased, while the increase of laser power gave rise to the maximum developed temperature. Finally, it was found that this manufacturing method is suitable for the polymerisation of thin films and sensors.

ACKNOWLEDGMENTS

The present work was conducted as part of a 3-year PhD research programme (by the first author) at the School of Materials, University of Manchester, and funded by the President's Doctoral Scholar (PDS) Awards scheme.

CONFLICT OF INTEREST

There is no conflict of interest to be declared.

ORCID

Asimina Manta  <https://orcid.org/0000-0002-6143-2275>

Constantinos Soutis  <https://orcid.org/0000-0002-1402-9838>

REFERENCES

1. Castro Neto AH, Guinea F, Peres NMRS, Novoselov KS, Geim AK. The electronic properties of graphene. *Rev Mod Phys*. 2009;81:109-162.
2. Katsnelson MI. Graphene: carbon in two dimensions. *Mater Today*. 2007;10:20-27.
3. Avouris P. Graphene: electronic and photonic properties and devices. *Nano Lett*. 2010;10:4285-4294.
4. Zhu SE, Yuan S, Janssen GCAM. Optical transmittance of multilayer graphene. *Epl*. 2014;108:1-4.
5. Zhu J, Liu QH, Lin T. Manipulating light absorption of graphene using plasmonic nanoparticles. *Nanoscale*. 2013;5:7785.
6. Liu X, Huang J, Wang X, Cheng G, He Y. Investigation of graphene nanofluid for high efficient solar steam generation. *Energy Procedia*. 2017;142:350-355.
7. Chen L, Xu C, Liu J, Fang X, Zhang Z. Optical absorption property and photo-thermal conversion performance of graphene oxide/water nanofluids with excellent dispersion stability. *Sol Energy*. 2017;148:17-24.
8. Wang N, Xu G, Li S, Zhang X. Thermal properties and solar collection characteristics of oil-based nanofluids with low graphene concentration. *Energy Procedia*. 2017;105:194-199.
9. Paschotta R. *Laser applications, Encyclopedia of Laser Physics and Technology*. Wiley-VCH; 2008. https://www.rp-photonics.com/laser_applications.html
10. Labudovic M, Hu D, Kovacevic R. Three-dimensional finite element modelling of laser surface modification. *Proc Inst Mech Eng Part B J Eng Manuf*. 2000;214:683-692.
11. Bachy B, Franke J. Simulation of laser structuring by three dimensional heat transfer model. *Int J Mater Metall Eng*. 2014;8:1723-1729.
12. Yu P, Yu S, Zhou W. Evaluation of thermal performance of graphene overcoat on multi-layered structure subject to laser heating. *Int Commun Heat Mass Transf*. 2015;68:27-31.
13. Manta A, Gresil M, Soutis C. Multi-scale finite element analysis of graphene/polymer nanocomposites electrical performance. *Proc VII Eur Cong Comput Methods Appl Sci Eng (ECCOMAS Congress 2016)*. 2016;1:1984-2002.
14. Manta A, Gresil M, Soutis C. Predictive model of graphene based polymer nanocomposites: electrical performance. *Appl Compos Mater*. 2017;24:281-300.
15. Manta A, Gresil M, Soutis C. Graphene in aerospace composites: characterising thermal response. *AIP Conf Proc*. 2018;1932:020001.
16. Manta A. *Design and Simulation of Graphene/Epoxy Nanocomposites: A Multi-Scale Approach on Mechanical, Thermal and Electrical Behaviour*. PhD Thesis: The University of Manchester; 2019.
17. Bernath A, Kärger L, Henning F. Accurate cure modeling for isothermal processing of fast curing epoxy resins. *Polymers*. 2016;8:1-19.
18. Pop E, Varshney V, Roy AK. Thermal properties of graphene: fundamentals and applications. *MRS Bull*. 2012;37:1273-1281.

How to cite this article: Manta A, Soutis C, Gresil M. Laser-aided curing of a GnP/epoxy nanocomposite optimised by multiscale finite element analysis. *Mat Design Process Comm*. 2019;1:e32. <https://doi.org/10.1002/mdp2.32>